A carbon budget for a naturally iron fertilized bloom in the Southern Ocean

Paul J. Morris[1,2] and Richard Sanders[1]

Received 13 January 2010; revised 28 November 2010; accepted 21 February 2011; published 8 July 2011.

[1] Subantarctic islands in the high-nutrient, low-chlorophyll (HNLC) Southern Ocean are natural sources of iron and stimulate blooms in their proximity, such as the one observed close to the Crozet Islands (52°E, 46°S). During 2004/2005, particulate organic carbon (POC) export was measured using the ^{234}Th technique in the Crozet bloom and compared with an HNLC control region. Initial results showed that iron release had no effect on daily POC export rates, thus any iron-driven enhancement in POC export was due to a longer export phase in the bloom region when compared to the control region. The duration of the export event was empirically estimated by closing the silicon budget, thus allowing seasonal POC export to be calculated by applying the export duration to the daily rates of POC export. This yields a seasonal estimate of POC export that is 3.6 times larger (range 1.9–7.1) in the iron-fertilized region than in the HNLC control region. These estimates of POC export were then compared to independent estimates of organic matter storage in the upper ocean, which are significant in both the HNLC and control regions. Overall, integrated POC export was significantly (approximately 50%) lower than estimated seasonal new production, the fraction of production that is supported by inputs of new nutrients. Finally, the sequestration efficiency, the numerical relationship between the supply of the limiting nutrient, iron, and the key ecosystem function of POC export at 100 m, is estimated to be 16,790 mol:mol.

Citation: Morris, P. J., and R. Sanders (2011), A carbon budget for a naturally iron fertilized bloom in the Southern Ocean, *Global Biogeochem. Cycles*, *25*, GB3004, doi:10.1029/2010GB003780.

1. Introduction

[2] The oceanic Biological Carbon Pump (BCP) is a significant component (ca. 11 Gt C yr^{-1}) of the global carbon cycle [*Prentice et al.*, 2001]. It consists mainly of the gravitational sinking of small particles, with the organic component ultimately derived from photosynthetic phytoplankton in the upper ocean, which use sunlight to fix carbon dioxide, water and nutrients. The geographical distribution of the BCP generally follows the distribution of phytoplankton biomass [*Falkowski et al.*, 1998; *Laws et al.*, 2000], itself regulated by the distribution of the macronutrients nitrate and phosphate. However, in some regions this correlation breaks down with these regions having high nutrient and low chlorophyll levels [*Boyd*, 2008]. Such areas, termed HNLC, are generally accepted to occur because production in these regions is limited by the availability of the micronutrient iron (Fe), required by phytoplankton for multiple cellular functions including photosynthesis, respiration and nitrate utilization [*Geider and La Roche*, 1994].

[3] The largest and most biogeochemically significant HNLC region is the Southern Ocean [*Tréguer et al.*, 1995]. Our knowledge regarding the role of Fe in regulating plant production, nutrient use and particulate organic carbon (POC) export in the Southern Ocean is substantially built on shipboard mesoscale Fe enrichment experiments, in which small patches of water were fertilized with Fe [*Boyd et al.*, 2007]. These experiments have provided unequivocal evidence that Fe is important in regulating plankton productivity, nutrient use and CO_2 drawdown. However, such experiments may be poor mimics of the long-term Fe fertilization that occurs in natural environments. Natural blooms generally last for months [*Blain et al.*, 2007; *Korb et al.*, 2008] and may be subject to macronutrient (silicate) limitation and grazing pressure in ways that deliberately induced mesoscale blooms are not. For these reasons an alternative strategy to infer the effects of long-term, large-scale Fe fertilization on the HNLC Southern Ocean has emerged. Based on the observation that some regions around islands or shallow topography have high chlorophyll levels it was hypothesized that the terrestrial release of dissolved Fe can stimulate phytoplanktonic photosynthesis and possibly POC export [*Holeton et al.*, 2005].

[4] In the austral summer of 2004/5, a 3 month oceanographic expedition to the region around the Crozet Islands set out to investigate the impact of natural Fe fertilization, the results of which are summarized by *Pollard et al.* [2009]. *Pollard et al.* [2009] used a novel silicon (Si) cycle scaling technique to transform daily rates of ^{234}Thorium-derived POC export into seasonal estimates. This manuscript describes the philosophy and implementation of the

[1]National Oceanography Centre, Southampton, University of Southampton, Southampton, UK.
[2]Now at Department of Marine Chemistry and Geochemistry, Woods Hole Oceanographic Institution, Woods Hole, Massachusetts, USA.

0886-6236/11/2010GB003780

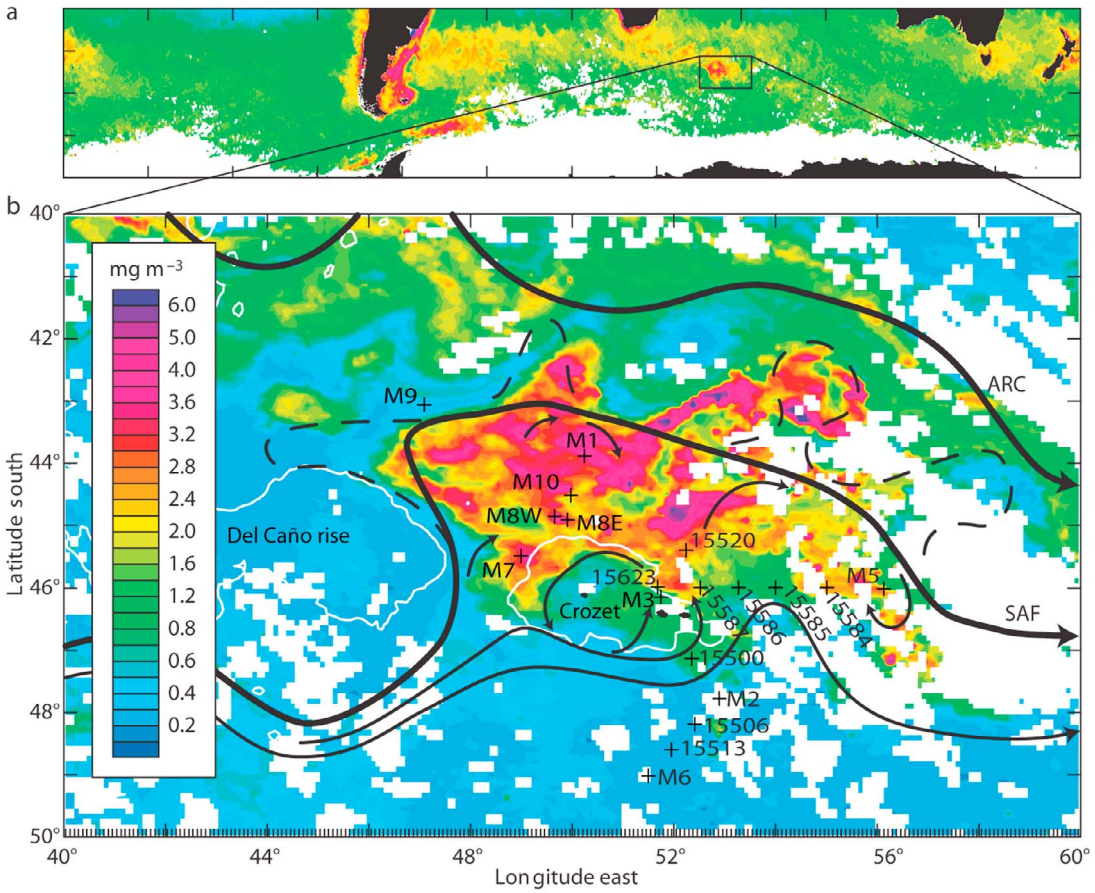

Figure 1. Satellite images of chl-*a*. (a) Chl-*a* distribution for the whole of the Southern Ocean in October and the location of the Crozet Islands. (b) Merged SeaWiFS/MODIS images of chl-*a* during an 8 day window (23–30 October 2004) at the peak of the bloom. Black lines denote the main eastward circulation [*Pollard et al.*, 2007b] of the Agulhas Return Current (ARC) and Subantarctic Front (SAF). Station locations (+) are labeled, white lines are 2000 m bathymetry contours and the main Crozet Islands are centered around 52°E, 46.4°S. This figure has been taken and modified from *Pollard et al.* [2009].

Si-scaling model and shows that there is an approximately 3.6-fold difference in POC export between the high-productivity bloom region and the HNLC control region. An important result from the model is that new production (NP) and POC export are not equivalent. This result will be discussed and validated by comparing it with estimates of other pools of organic matter in the upper ocean.

[5] The critical result presented by *Pollard et al.* [2009] is the estimate of the sequestration efficiency, the ratio of POC exported per unit Fe added (mol:mol). *Pollard et al.* [2009] derived a value of about 17,200 at 100 m, 2orders of magnitude lower than that derived by *Blain et al.* [2007] in the only comparable study (KEOPS). However, the analysis of *Pollard et al.* [2009] did not consider some key terms, thus an updated sequestration efficiency will be calculated.

2. Methods

2.1. Study Site and Sampling Strategy

[6] The geographical setting of the Crozet archipelago, its hydrographic surroundings and suitability for studying the island effect in an HNLC region are covered by *Morris et al.* [2007] and *Pollard et al.* [2007b]. Sampling for the CROZEX project took place from November 2004 to January 2005 on two cruises onboard the RRS *Discovery*, cruises D285 and D286, which will be referred to as leg 1 and 2, respectively, from hereon [*Pollard et al.*, 2007a; *Pollard and Sanders*, 2006]. Sampling was focused on categorizing the main bloom area in the north of the study region. However, these observations were complemented with observations in the southern, nonbloom control region. Stations were numbered using the sequential Discovery station number [*Discovery Reports*, 1929], however, major process stations were also designated with an M number (Figure 1). Repeated occupations of the same M station were denoted by decimals. Stations were regionalized into north (N), center (C), south (S), east (E) and west (W) depending on their locations (Table S1).[1]

2.2. Analytical Methods

2.2.1. Total Thorium and the Stand-Alone Pump System

[7] Determination of total ^{234}Thorium (^{234}Th) using the 10 L MnO_2 precipitation technique was based on the

[1] Auxiliary materials are available with the HTML. doi:10.1029/2010GB003780.

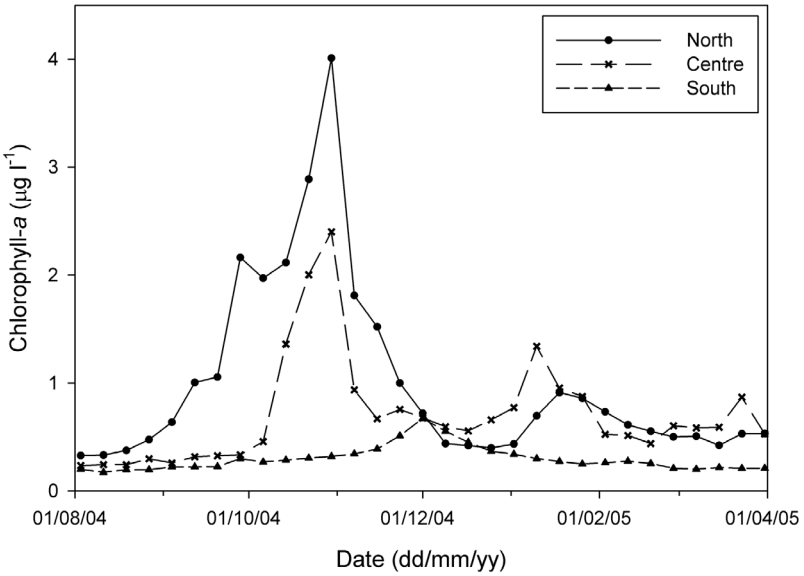

Figure 2. Remotely sensed temporal progression of chl-*a* in the north, center and south. Taken from *Venables et al.* [2007].

method of *Rutgers van der Loeff and Moore* [1999], and was extensively described by *Morris et al.* [2007]. Likewise, the collection of large particles (>53 μm) with in situ pumps to determine carbon-to-thorium ratios (C:Th) was also described by *Morris et al.* [2007]. To take advantage of elemental-to-thorium ratios to determine other elemental fluxes, the biogenic silica-to-thorium ratio (BSi:Th) was also measured. BSi was measured on particles collected by a Challenger Oceanic stand-alone pump system (SAPS), in situ pumps that are capable of filtering large volumes of seawater through large-diameter (293 mm) filters. Briefly, SAPS splits for BSi were filtered through 0.4 μm polycarbonate filters, which were then stored at −20°C for subsequent analysis. BSi was dissolved in NaOH at 100°C for 3 h, then mixed with molybdate before finally being reduced to form a blue compound that was measured on a spectrophotometer (Hitachi U-2000] at 810 nm. Details of BSi analysis can be found in the works of *Salter et al.* [2007] and *Salter* [2007], and was based on the method of *Mortlock and Froelich* [1989].

2.2.2. Nutrients, POC/N, BSi, Chl-*a* and TON

[8] Nutrient samples for nitrate + nitrite (nitrate from hereon) and silicate were collected and analyzed onboard ship using the method described by *Sanders et al.* [2007], which is in turn based on the methods by *Kirkwood* [1996]. The nutrient analyzer (Skalar SansPlus) was controlled by a computer running the FlowAccess software that automatically integrates sample peak heights and calculates the nutrient concentration based on a predefined calibration regime. Particulate organic carbon/nitrogen (POC/N) samples were collected by filtering 1–2 L of seawater through precombusted 25 mm GF/F filters, which were then stored at −20°C. POC/N samples were analyzed by high-temperature combustion (Finnegan Flash EA1112 Elemental Analyzer) after removal of carbonate by fuming with sulphurous acid [*Ehrhardt and Koeve*, 1999; *Hilton et al.*, 1986; *Verardo et al.*, 1990], and had an RSD error of 28% and 18% for POC and PON, respectively. BSi samples were collected by filtering 500 mL of seawater through 0.4 μm polycarbonate filters, which were then dried, mixed with NaOH at 60°C for 2 h to dissolve the BSi and then neutralized with HCl. The resultant aqueous sample was then run on the silicate channel of the nutrient analyzer while at sea. Chlorophyll-*a* (chl-*a*) analysis is outlined by *Moore et al.* [2007b] and is based on that of *Welschmeyer* [1994]. Total organic nitrogen (TON) samples were collected directly from the CTD into 60 mL Sterilin® pots prewashed with sample and then stored at −20°C until subsequent analysis using the UV photooxidation method described by *Sanders and Jickells* [2000], and had an RSD error of 3%. As these samples were not filtered they will be considered as total organic nitrogen samples, rather than dissolved organic nitrogen (DON) samples.

2.3. General Synopsis

[9] As with previous years, an intense bloom lasting about 120 days was observed to the north of the islands with chl-*a* levels peaking at 4 μg L^{-1} at the start of November. To the south of the islands no such bloom was observed, again consistent with previous years, although at the start of November for about 60 days a small increase in surface chl-*a* of up to 0.7 μg L^{-1} was observed (Figure 2) [*Venables et al.*, 2007]. To clarify terminology for the different study regions, the area to the north of the Crozet Plateau where the main bloom event occurs will be referred to as either: northern, high productivity or bloom region. The area to the south of the Crozet Plateau will be referred to as either: southern, low productivity, nonbloom, HNLC or control region.

3. Silicon-Scaling Model: Rationale

[10] It was necessary to construct a scaling model because the individual postbloom daily rates of ^{234}Th-derived POC export (^{234}Th-POCex), which were similar in the HNLC and

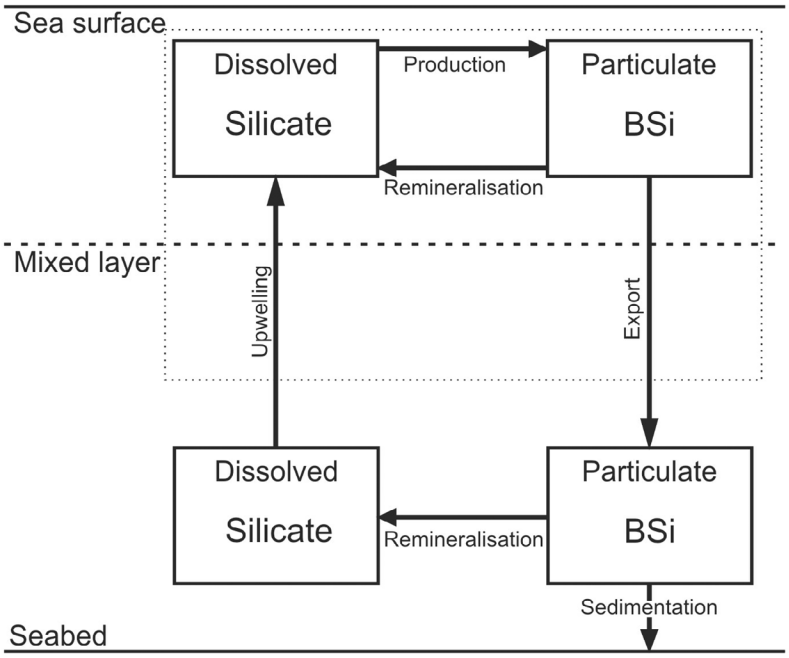

Figure 3. Schematic of the marine Si cycle showing the major pools and fluxes between them. The part of the marine Si cycle to be used to temporally integrate daily rates of ^{234}Th-Cex is contained within the dotted box.

bloom regions [*Morris et al.*, 2007], needed to be scaled by an estimate of export duration. This allowed an evaluation of whether time-integrated POC export in the two regions was similar. Daily rates of ^{234}Th-derived export for POC and BSi export were calculated by multiplying the measured ^{234}Th export by the C:Th and BSi:Th ratios, respectively. In essence, the model asked the question: "How many days does the observed export of BSi need to persist in order to close the Si budget?" The results from this question were then applied to the measured daily rates of POC export in each region. The Si (rather than the carbon) cycle was used because if the carbon cycle was used, then the calculation would become circular and there would be no independent way of validating the POC export estimate produced. The scaling model attempts to calculate seasonal export estimates, however in reality it can only integrate up to the date that each station was sampled. Given that the CROZEX cruises sampled toward the end of the main bloom event, temporal integrations of export should be approaching a seasonal value.

[11] Silicon is a highly important element for several plankton functional groups including diatoms [*Tréguer et al.*, 1995], silicoflagellates and radiolarians with diatoms recorded as the dominant opaline functional group in the Southern Ocean [*El-Sayed et al.*, 1983]. Diatoms can either be exported directly out of the euphotic layer or are grazed by zooplankton such as copepods. Importantly, grazed diatom frustules are inert in the guts of copepods [*Dagg et al.*, 2003; *Tande*, 1985] and thus Si is not assimilated into higher trophic levels, as happens with carbon and nitrogen [*Brzezinski and Nelson*, 1989; *Dugdale et al.*, 1995]. Instead, ingested BSi is efficiently packaged in faecal pellets that readily sink at rates in excess of 100 m d^{-1} [*Small et al.*, 1979] thus allowing efficient export to mesopelagic depths [*Dagg et al.*, 2003]. BSi only returns Si to the dissolved inorganic phase, silicate, through the process of dissolution [*Broecker and Peng*, 1982]. Consequently, the Southern Ocean is a major sedimentary sink of Si, accounting for up to 75% of global deposits [*Calvert*, 1983; *DeMaster*, 1981; *Ledford-Hoffman et al.*, 1986; *Tréguer and Jacques*, 1986], and the silicate pump, driven through the export of diatoms, is therefore a critical component of the Si cycle [*Dugdale et al.*, 1995]. Overall, Si has a simpler cycle than carbon (Figure 3), which is easier to understand and close, and can thus be used to independently constrain the carbon cycle.

3.1. Model Description

[12] The model functions on the principle of calculating the theoretical export of BSi that must have occurred up to the date of sampling, based on the drawdown of dissolved silicate (DSi), corrected for any increase in mixed layer stocks of BSi that have not yet been exported [*Morris*, 2008]. This is then divided by the measured export of BSi to estimate the number of days that export must have persisted for. The model builds upon and explains the details of the Si-scaling model presented by *Pollard et al.* [2009], but has the addition of a DSi upwelling component to correct for additional DSi that has entered the mixed layer during the bloom season. Figure 3 shows a schematic representation of the processes considered.

3.1.1. Drawdown of Dissolved Silicate

[13] The seasonal drawdown of DSi at each station (ΔDSi) was calculated by assuming that the winter concentration of DSi found in the top 100 m of the water column can be extrapolated from the measured summer concentration at 100 m. A justification for using 100 m as the integration depth is given by *Sanders et al.* [2007] and *Bakker et al.* [2007]. The amount of DSi that was available at the start of

the bloom season (DSi_w) was calculated using equation (1), where DSi_{100} is the summer concentration at 100 m and *dz* is the depth of integration. The 0–100 m summer inventory of DSi when each station was sampled (DSi_s) was then calculated using equation (2), where *dz* is the layer thickness and $\overline{DSi}$ is the averaged DSi concentration over each integral layer, expressed by equation (3). The seasonal ΔDSi was then calculated with equation (4).

$$DSi_w = \int_0^z dz \times DSi_{100} \tag{1}$$

$$DSi_s = \int_0^z dz \times \overline{DSi} \tag{2}$$

$$\overline{DSi} = \frac{(DSi_1 + DSi_2)}{2} \tag{3}$$

$$\Delta DSi = DSi_w - DSi_s \tag{4}$$

3.1.2. Accumulation of Biogenic Silica

[14] The seasonal accumulation of BSi in the mixed layer, which acts to reduce the amount of BSi available for export, was assessed with inventories of BSi. 100 m summer inventories (BSi_s) were corrected with an estimate of the winter standing stock of BSi (BSi_w). Winter standing stocks across the whole study area were assumed to equal the 100 m inventories measured in the southern region on leg 1. This assumption was based on remotely sensed chl-*a* data, which shows near identical biomass levels in the bloom and control regions in August [*Venables et al.*, 2007]. BSi inventories were calculated using the same approach as equations (2) and (3) and is summarized by equation (5) where $\overline{BSi}$ is the average BSi concentration over each integral layer akin to equation (3). ΔBSi was then calculated by equation (6) where BSi_w was equal to the average of BSi inventories of the four southern stations on leg 1 (131 mmol Si m^{-2}).

$$BSi = \int_0^z dz \times \overline{BSi} \tag{5}$$

$$\Delta BSi = BSi_s - BSi_w \tag{6}$$

3.1.3. Upwelling of Dissolved Silicate

[15] To assess the upwelling of DSi (DSi_{up}) in to the mixed layer, the concentration gradient of DSi ($\partial DSi/\partial z$) was calculated based on the DSi concentrations of samples taken adjacent to the 100 m depth horizon, which were typically in the range of 80–130 m. A vertical turbulent diffusion coefficient (K_z) was then used according to equation (7). A K_z of 0.38 cm^2 s^{-1}, measured using LADCP data, was taken as the average K_z over 100–200 m from *Charette et al.* [2007, Figure 6]. The daily rates of upwelling DSi were then multiplied by the bloom length unique to each station, which is the length of time that the bloom had persisted at each station until the time that that station was sampled. This was determined using the progression of chl-*a* in Figure 2. DSi_{up} was, on average, 8% of seasonal ΔDSi, a small but significant contributor to mixed layer DSi inventories.

$$DSi_{up} = K_z \times \left(\frac{\partial DSi}{\partial z}\right) \tag{7}$$

3.1.4. Theoretical BSi Export and Calculation of Seasonal Carbon Export

[16] By combining the results of equations (4), (6) and (7) the theoretical total BSi that had been exported up to the date of sampling ($BSiex_t$) can be calculated as the sum of ΔDSi and DSi_{up} minus the storage of ΔBSi (equation (8)). After calculating $BSiex_t$ the mean was taken for each region. From these it was then calculated how long in days (*t*) the regional average daily rates of ^{234}Th-derived BSi export (^{234}Th-BSiex) would have needed to persist for to account for the calculated theoretical $BSiex_t$ (equation (9)). The value of *t* was calculated for each region: north, center and south, and then *t* was applied to the average ^{234}Th-POCex in each region to calculate seasonally integrated POC export ($POCex_t$) (equation (10)).

$$BSiex_t = \Delta DSi + DSi_{up} - \Delta BSi \tag{8}$$

$$t = \frac{BSiex_t}{^{234}Th{-}BSiex} \tag{9}$$

$$POCex_t = {}^{234}Th{-}POCex \times t \tag{10}$$

Clearly there is some variability in the Si:C ratio of the exported material over the course of the observations (Table S2). If the mean Si:C ratios of the particles used to calculate the duration of export in equation (9) differ significantly from the seasonally and spatially integrated mean Si:C ratio of the exported material, then applying the durations of export derived from closing the Si budget may be inappropriate. The only realistic way to determine whether this is an appropriate strategy is to determine whether the estimates of POC export derived from the Si-scaling model are consistent with independent estimates of NP. There is also a marked north-south difference in the Si:C ratio of exported particles: 0.5 north versus 1.7 south. This is consistent with the known plasticity of diatom Si:C ratios as a function of Fe limitation [*Hutchins and Bruland*, 1998].

3.2. Data Input and Model Results

[17] The 100 m inventories of DSi_w, DSi_s, BSi_s, used in the model are presented in Table 1, together with daily DSi_{up} and bloom length. The $BSiex_t$ at each station, which results from equation (8), is shown in the last column of Table 1. When the regional averages (bold values) are divided by the daily rates of ^{234}Th-BSiex, the duration of the export event in each region can be calculated (Table 2). Seasonally integrated POC export is then calculated by multiplying the average daily rates of POC export by the duration of the export event (Table 2 and equation (10)). Table S2 shows the calculation of daily rates of ^{234}Th-BSiex.

Table 1. The 100 m Integrated Inventories of DSi_w, DSi_s, BSi_s, DSi_{up}, Bloom Length, and $BSiex_t$ Available for Export[a]

Station	DSi_w	DSi_s	BSi_s[b]	DSi_{up}[c]	Bloom length (d)	$BSiex_t$
	(mmol m^{-2})			(mmol m^{-2} d^{-1})		(mmol m^{-2})
			North			
M1	1494 ± 50	307 ± 13	278 ± 22	1.00	71	1111
M8E	1304 ± 35	589 ± 13	120 ± 9	0.45	90	767
M8W	826 ± 18	206 ± 5	194 ± 15	0.71	92	623
M9.1	1244 ± 33	456 ± 12	115 ± 9	0.30	93	832
M9.2	663 ± 18	194 ± 5	59 ± 5	0.58	109	604
M10.1	1142 ± 30	462 ± 11	239 ± 20	0.62	110	641
					Mean	**763 ± 79**
			Center			
M3.1	734 ± 20	699 ± 15	374 ± 15	0.13	43	−202[d]
M3.3	1162 ± 31	927 ± 20	307 ± 26	0.29	55	75
M3.4	1015 ± 27	364 ± 9	334 ± 27	0.54	82	492
M3.5	1117 ± 30	492 ± 11	104 ± 9	0.47	91	695
M3.6	1705 ± 45	810 ± 20	232 ± 19	0.39	100	833
M3.7	1766 ± 50	790 ± 25	196 ± 16	0.37	101	949
M3.8	2046 ± 55	829 ± 22	218 ± 18	0.40	103	1171
					Mean	**703 ± 157**
			South			
M3.2[e]	1936 ± 55	1540 ± 41	219 ± 18	0.23	17	312
M2.1	1832 ± 49	1674 ± 36	97 ± 10	0.39	19	199
M6.1	1979 ± 53	1836 ± 41	140 ± 12	0.15	21	137
M6.2	1136 ± 30	319 ± 8	311 ± 25	0.81	63	688
M2.2	1183 ± 32	378 ± 10	292 ± 24	0.69	66	690
					Mean	**405 ± 119**
					Mean leg 2 stations only[f]	**689 ± 1**

[a]Errors for individual stations are propagated 1 σ analytical uncertainties, and the values in bold are regional averages and associated standard errors.
[b]BSi has to be corrected by the winter stock (131 mmol Si m^{-2}, sd 39 mmol Si $^{-2}$, n = 4).
[c]Upwelling has to be factored by the bloom length and has a factor of 3 nominal uncertainty.
[d]M3.1 was excluded from this point onward because it generated a negative number.
[e]Station M3.2 has been grouped with the southern stations because it was shown to be influenced by water from the south [*Pollard et al.* 2007b].
[f]For the southern region, only leg 2 stations were carried forward for the calculation of export duration. On leg 1 the bulk particulate export had not occurred in this region, and for the analysis to remain consistent with the other regions, only the southern stations, which were sampled after the southern bloom, were used.

[18] Export durations of 87, 56 and 24 days are calculated for the north, center and south regions, respectively (Table 2). These are on average slightly less, but broadly consistent with, the lengths of bloom in each region (Table 1). These export durations thus yield seasonal estimates of $POCex_t$ of 1.44 and 0.40 mol C m^{-2} in the northern and southern regions, respectively. Uncertainty calculations of all the terms in Table 2 are given in the respective footnote. Given that this is as close to a seasonal estimate of POC export that might be obtained for the CROZEX region, then an obvious comparison to make is with the other measurements of NP. To clarify the term NP, it can be viewed as the production that arises from the input of new nutrients into the euphotic zone such as upwelled nutrient rich deep water, atmospheric deposition, riverine inputs and nitrogen fixation [*Dugdale and Goering*, 1967].

[19] There currently exist three independent estimates of NP for the CROZEX bloom. *Sanders et al.* [2007] report seasonal nitrate deficits of 4.16 mol C m^{-2} in the northern region and 1.25 mol C m^{-2} in the southern region. *Lucas et al.* [2007] report estimates of ^{15}N NP ranging from 2.69 mol C m^{-2} to 0.42 mol C m^{-2} in the north and south, respectively. Finally, *Bakker et al.* [2007] report dissolved inorganic carbon deficits of 2.5–3.4 mol C m^{-2} in the north, dropping to

Table 2. Regional ^{234}Th-BSiex and Model-Predicted $BSiex_t$, Used to Calculate a Scaling Factor to Recalibrate the ^{234}Th-Cex to Give $POCex_t$[a]

Region	^{234}Th-BSiex (mmol m^{-2} d^{-1})	$BSiex_t$ (mmol m^{-2})	Duration of Export (days)	^{234}Th-POCex (mmol m^{-2} d^{-1})	$POCex_t$ (mmol m^{-2})
North	8.8 ± 1.9	763 ± 79	87 (64–123)	16.5 ± 1.7	1437 (949–2239)
Center	12.7 ± 1.1	703 ± 157	56 (40–74)	13.9 ± 1.4	771 (495–1137)
South	28.9 ± 2.5	689 ± 1	24 (22–26)	16.6 ± 1.4	396 (316–491)

[a]Uncertainties of all terms were derived as follows: ^{234}Th-POCex and ^{234}Th-BSiex are regional averages and their associated standard errors carried forward from Table S2. $BSiex_t$, the theoretical amount of Si available for export, are regional averages and their standard errors that result from the Si-scaling model presented in Table 1. The duration of export is given a range by reapplying equation (9) to the upper and lower standard errors of ^{234}Th-BSiex and $BSiex_t$. In turn, $POCex_t$ is given a range by reapplying equation (10) to the upper and lower standard error estimates of ^{234}Th-POCex to the range in the duration of export.

1.3 mol C m^{-2} in the south. All three of these NP estimates are broadly consistent with each other and follow the same north-south trend in POC export that has been revealed by the Si-scaling model.

[20] However, these estimates of NP appear to be systematically bigger than the estimates of POC export presented in Table 2 by a factor of about 1.8–2.8 in the northern region and 1.1–3.3 in the southern region. This is an interesting observation because a central dogma of biological oceanography is that over appropriate time and space scales NP and particle export should balance [*Dugdale and Goering*, 1967; *Eppley and Peterson*, 1979]. Although the magnitude of the offset between NP and export production varies depending on which methods are compared, the offset appears to be a consistent and thus robust feature of the CROZEX study site. A possible reason for the offset could result from flaws within the Si-scaling method. For example, there may be a mismatch between the mean Si:C ratios in exported particles when compared to the spatial mean of this ratio. Alternatively, there could be a real difference between new and export production that may be potentially caused by an accumulation of dissolved organic matter (DOM) in the upper ocean. To address this point an assessment of the upper ocean organic matter pools has to be made.

4. Upper Ocean Standing Stocks

4.1. Total Organic Nitrogen

[21] Figure 4a shows 0–100 m integrated TON compared to chl-*a* (Table S1). The Model II regression between TON and chl-*a* is TON = 1.50 x chl-*a* + 245 (r^2 = 0.40, p = <0.01, n = 26). Relationships of this sort are not common in the literature, but one example reported by *Bode et al.* [2001] from shelf waters off northern Spain agrees well once converted to comparable units: DON = 1.18 × chl-*a* + 421, (r^2 = 0.48). The higher intercept observed by *Bode et al.* [2001] is unsurprising because their study was conducted in coastal waters where higher levels of background organic matter might be expected.

[22] To assess the fraction of TON that has accumulated from NP, a comparison between TON inventories and nitrate drawdown (ΔNO_3^-) can be made. ΔNO_3^- were calculated as the difference between the measured inventory of summer NO_3^- (NO_{3s}^-) and an inferred winter inventory of NO_3^- (NO_{3w}^-), using the same approach as *Sanders et al.* [2007]. ΔNO_3^- were recalculated to ensure consistent integration techniques with other data sets within this study. NO_{3w}^- was inferred by assuming that the 0–100 m concentration of NO_3^- was the same as the summer 100 m concentration. Nitrate NP, (ΔNO_3^- NP), calculated as the amount of nitrate drawdown from the end of winter mixing until the date of sampling, is shown in Table S1. The relationship between 100 m inventories of TON and ΔNO_3^- NP is shown in Figure 5a. The regression is TON = 0.46 × ΔNO_3^- + 256 (r^2 = 0.43, p = <0.01, n = 26), suggesting that ΔNO_3^- is directly correlated with TON concentrations over the range of conditions sampled and that 46 ± 7% of the NO_3^- removed through NP is entering the TON pool. This is higher than estimates of DOM release reported in the literature, which range from 0%–37% (Table 3).

[23] An extensive investigation of stocks and dynamics of DOM in the Ross Sea over multiseason sampling found that 10% and 11% of NP was released as DON and dissolved organic carbon (DOC), respectively [*Carlson et al.*, 2000]. In contrast, during a transect in the Polar Frontal region along 6°W in October and November 1992, no evidence of DOM buildup was recorded [*Kähler et al.*, 1997]. *Bakker et al.* [2006] calculated inferred DOC release after formulating a carbon budget of the SOIREE bloom and estimated that DOC release constituted 8%–37% of NP. In the Irminger Basin, North Atlantic, *Sanders et al.* [2005] estimated that 30% of ΔNO_3^- NP was accounted for in the DON pool. *Hu and Smith* [1998] also note that between 8% and 19% of NO_3^- assimilated by *Phaeocystis* cultures and natural phytoplankton assemblages in the Ross Sea, Southern Ocean was released as DON. Mesocosm experiments in high-latitude regions have also shown similar effects, with 6%–22% of total nitrogen uptake (mostly NO_3^-) recoverable as new DON [*Conan et al.*, 2007].

[24] Overall DOM release resulting from ΔNO_3^- NP seems to be a consistent feature over a wide range of conditions with fractions released ranging from 0%–37% (Table 3), which is lower than the fraction estimated here of 46%. A possible explanation for this difference is that the CROZEX samples were not filtered and thus may have contained a particulate organic matter (POM) fraction. This will now be investigated.

4.2. Particulate Organic Carbon and Nitrogen

[25] Standing stocks of 0–100 m integrated, POC and PON are shown plotted against chl-*a* in Figures 4b and 4c, respectively. The regression lines are Model II and have an r^2 in the range of 0.46–0.47, which are all significant at the 1% confidence level. The POC to chl-*a* ratio (POC:chl-*a*) is an indicator of Fe limitation, and tends to increase with increasing Fe stress as phytoplankton become depleted in chl-*a* [*Boyd et al.*, 2000; *Geider and La Roche*, 1994; *Greene et al.*, 1991; *Hoffmann et al.*, 2006].

[26] The regression of Figure 4b, using the secondary axis, is: POC = 52.13 × chl-*a* + 5394, (r^2 = 0.46, p = <0.01, n = 21). Taking the reciprocal of the gradient (1/52) reveals that overall chl-*a* constitutes about 2% of total POC on a weight for weight basis. However, the mean POC:chl-*a* ratios in northern and southern regions are 136 and 204, respectively, and a *t* test shows that these means are statistically different (p = <0.02). This provides evidence for enhanced chlorosis in the nonbloom region and supports the conclusion of increased Fe limitation in the southern region reported by others involved with direct biological measurements on CROZEX [*Lucas et al.*, 2007; *Moore et al.*, 2007a, 2007b; *Seeyave et al.*, 2007; *Zubkov et al.*, 2007]. This observed trend also agrees well with on-deck Fe perturbation experiments conducted by *Moore et al.* [2007b] who showed that Fe amended incubations decreased algal POC:chl-*a* by a factor of 2 when compared to Fe limited incubations.

[27] The relationship between PON and ΔNO_3^- NP is shown in Figure 5b. It appears to be nonlinear with a quadratic regression fitting the data (r^2 = 0.69, p = <0.01, n = 21) better than a linear regression (r^2 = 0.58, p = <0.01, n = 21). The general shape of the quadratic curve suggests relatively constant levels of PON occur as ΔNO_3^- NP increases up to about 250 mmol N m^{-2}. Above 250 mmol N m^{-2} PON

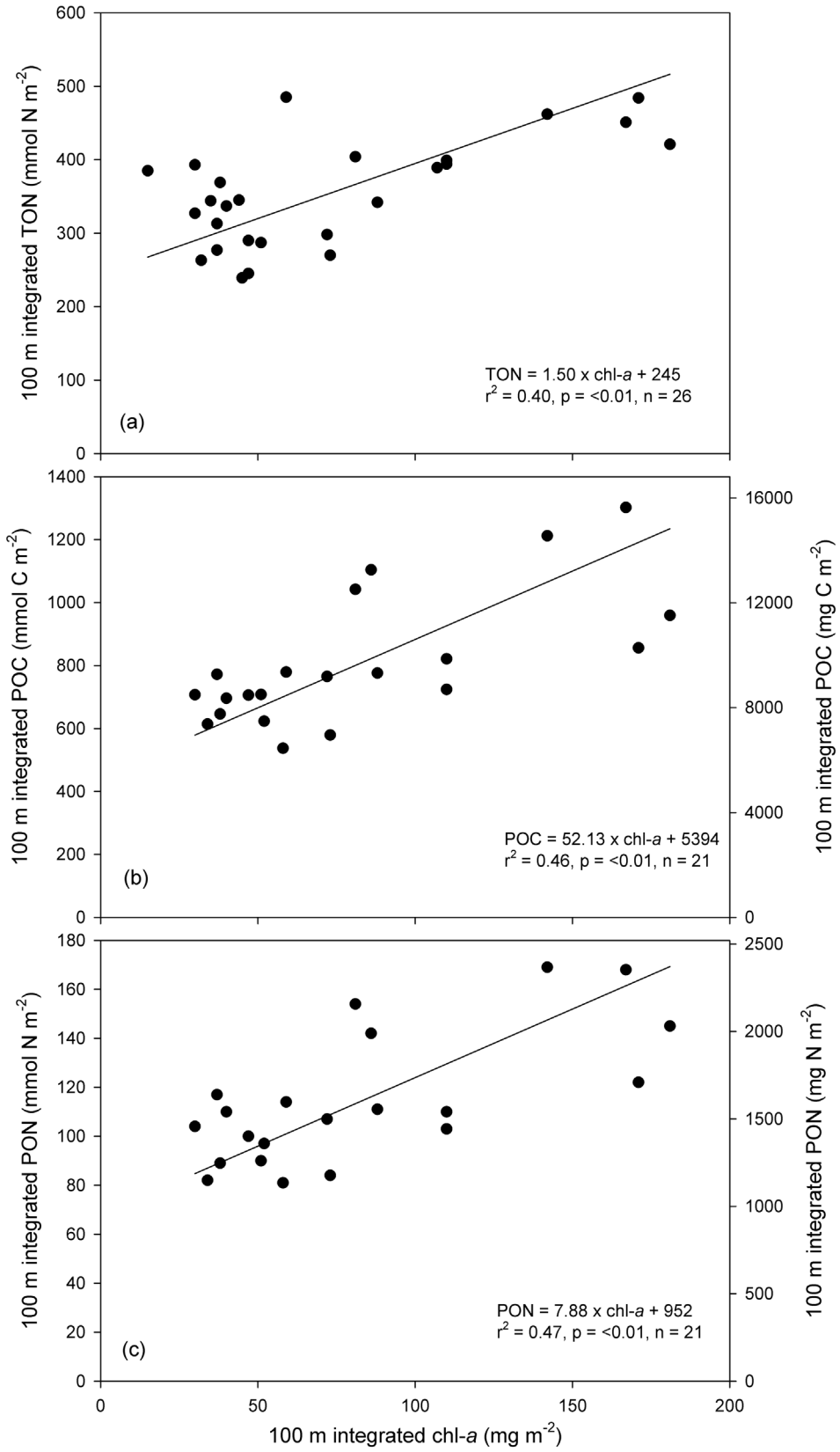

Figure 4. Relationships of 100 m integrated (a) TON, (b) POC, and (c) PON with chl-*a*. Solid lines are Model II regressions. Regressions for POC and PON take units from the secondary, right hand axis.

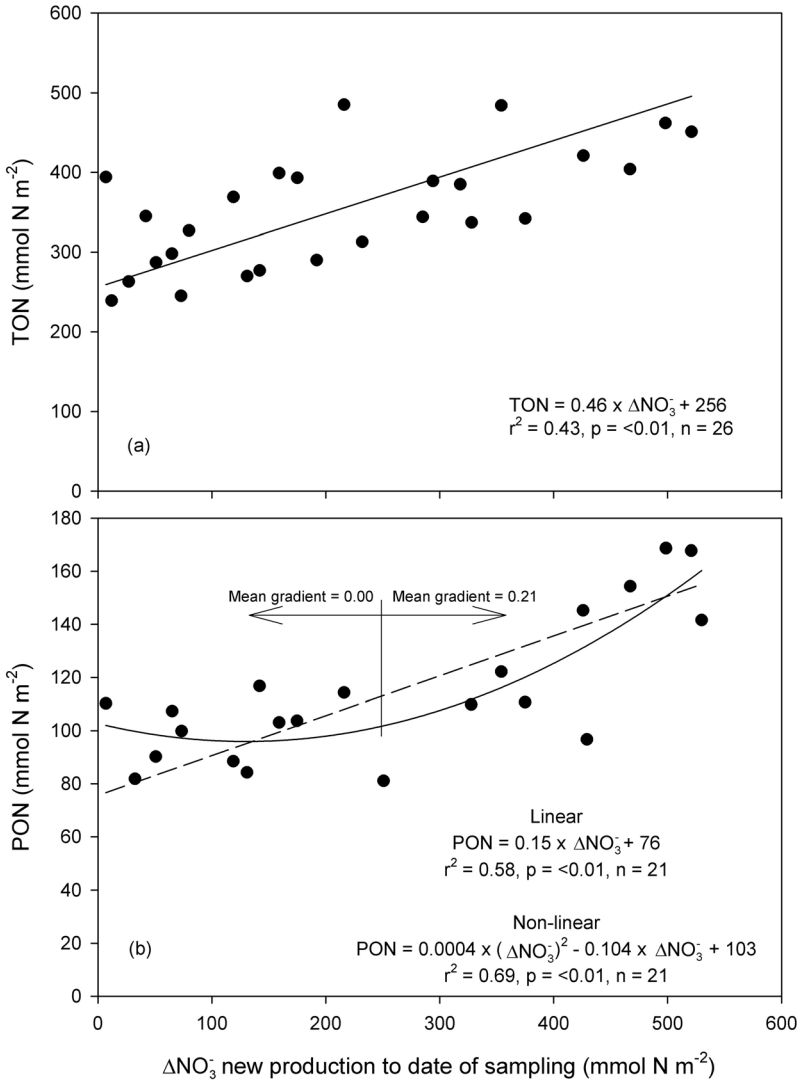

Figure 5. Relationships between 100 m integrated ΔNO_3^- NP up to the date of sampling and (a) TON and (b) PON. Solid line in Figure 5a is a Model II regression. The solid line in Figure 5b is a nonlinear quadratic regression with mean gradients above and below 250 mmol N m^{-2}. Dashed line in Figure 5b is the Model II linear regression for comparison.

increases approximately linearly with ΔNO_3^- NP. Using the nonlinear equation, the calculated 100 m inventory of PON at ΔNO_3^- NP = 250 mmol N m^{-2} is 102 mmol N m^{-2}. According to Figure 4c, 102 mmol N m^{-2} corresponds to a 100 m chl-*a* inventory of 61 mg m^{-2}.

[28] Interestingly, when the surface chl-*a* concentration is inferred from a 100 m chl-*a* inventory of 61 mg m^{-2} using the relationship between surface chl-*a* (chl-a_s) and 100 m integrated chl-*a* (chl-a_i) a value of 0.62 μg L^{-1} is returned (Figure 6). This is similar to the maximum surface chl-*a* concentration (0.67 μg L^{-1}) remotely sensed in the southern region at the peak of the bloom [*Venables et al.*, 2007] (see also Figure 2). This implies that estimates of ΔNO_3^- NP of <250 mmol N m^{-2} are representative of nonbloom conditions, and estimates of ΔNO_3^- NP of >250 mmol N m^{-2} are representative of bloom conditions.

[29] By using a moving window of 5 units of ΔNO_3^- NP, the average gradient of the nonlinear curve was calculated for areas of high and low ΔNO_3^- NP, which represent the northern bloom and southern HNLC stations, respectively. This analysis gives average gradients of 0.21 and 0.00 and means that PON accounts for about 21% and 0% of ΔNO_3^- NP in the north and south, respectively (Figure 5b).

[30] The accumulation of POM in the Southern Ocean during spring and summer is well documented [*Bakker*, 1998; *Bakker et al.*, 2006, 1997; *El-Sayed et al.*, 1983; *Nelson and Smith*, 1986; *Smith and Gordon*, 1997; *Smith et al.*, 1996; *Sweeney et al.*, 2000; *Wilson et al.*, 1986]. Of these, several studies have made estimates of the accumulation of POM from NP (Table 3). *Bakker et al.* [1997] estimated 47% on a transect during the austral spring along 6°W in the Polar Frontal Region. This estimate was later revised to 57% by *Bakker* [1998]. *Sweeney et al.* [2000] estimated ≈74% in the

Table 3. The Proportion of Newly Produced Organic Material Accounted for as DOM and POM for Various High-Latitude Studies

Study	Proportion of NP (%)	Reference
	DOM	
Ross Sea	10	*Carlson et al.* [2000]
Polar Frontal region	0	*Kähler et al.* 1997
SOIREE	8–37	*Bakker et al.* 2006
Irminger Basin	30	*Sanders et al.* 2005
Ross Sea	8–19	*Hu and Smith* [1998]
Mesocosms	6–22	*Conan et al.* [2007]
Range	0–37	
CROZEX		
+Fe	46	This study
-Fe	46	This study
	POM	
Ross Sea	74	*Sweeney et al.* [2000]
Polar Frontal region	57	*Bakker* [1998]
SOIREE	41	*Bakker et al.* [2006]
Range	41–74	
CROZEX		
+Fe	21	This study
-Fe	0	This study

Ross Sea during two cruises in late spring and summer; and results from SOIREE estimated 41% [*Bakker et al.*, 2006]. In comparison to these estimates CROZEX appears to be on the low side.

5. Discussion

5.1. The CROZEX Carbon Budget

[31] A primary objective of the CROZEX project was to assess the impact that natural Fe fertilization has on POC export from the euphotic zone. This was attempted with the ^{234}Th technique and led to the unexpected result that daily rates of POC export were not significantly stimulated by the large phytoplankton bloom in the north compared to the small bloom in the southern HNLC region [*Morris et al.*, 2007]. This result may have arisen from insufficient sampling at the peak of the bloom, or it may be a real result and the case that high-biomass regimes in the Southern Ocean do not export proportional amounts of POC [*Jacquet et al.*, 2008; *Lam and Bishop*, 2007; *Savoye et al.*, 2008]. Further work is required to examine this hypothesis. Despite this, an estimate of seasonal POC export was calculated via the Si-scaling model, which is consistent with the trend in NP, albeit persistently lower. Therefore the remainder of the discussion will address the difference in new and export production, using Figure 7 as a conceptual framework.

[32] Figure 7 draws together and summarizes information on seasonally integrated new production (ΔNO_3^- NP), seasonally integrated POC export, and the fluxes of organic material into the upper ocean standing stock. Integrated total primary production (TPP) was estimated via seasonal integrations of remotely sensed primary production. TPP was obtained via an empirical regression of surface chl-*a* to column-integrated primary production estimated using the ^{14}C technique [*Sanders et al.*, 2007]. Si-scaled POC export has been taken from Table 2 and ΔNO_3^- NP are regional averages from Table S1. Fluxes of organic material into the upper ocean standing stocks are taken from Figure 5. Total organic carbon (TOC) is considered to be both dissolved and particulate because the samples were not filtered; consequently POC is presented as a fraction of TOC. The exact partitioning of material between these pools is a little subjective as the larger uncertainty is in the PON measurements (18%); however the accuracy of the TON measurements is better (3% as stated earlier). For a carbon budget to be formulated from the nitrogen-based information: ΔNO_3^- NP and Figure 5, the assumption that carbon and nitrogen are behaving proportionally has to be met. For CROZEX, this issue was discussed by *Sanders et al.* [2007] and it was concluded that the use of a Redfield ratio of 6.6 is a fair assumption to make.

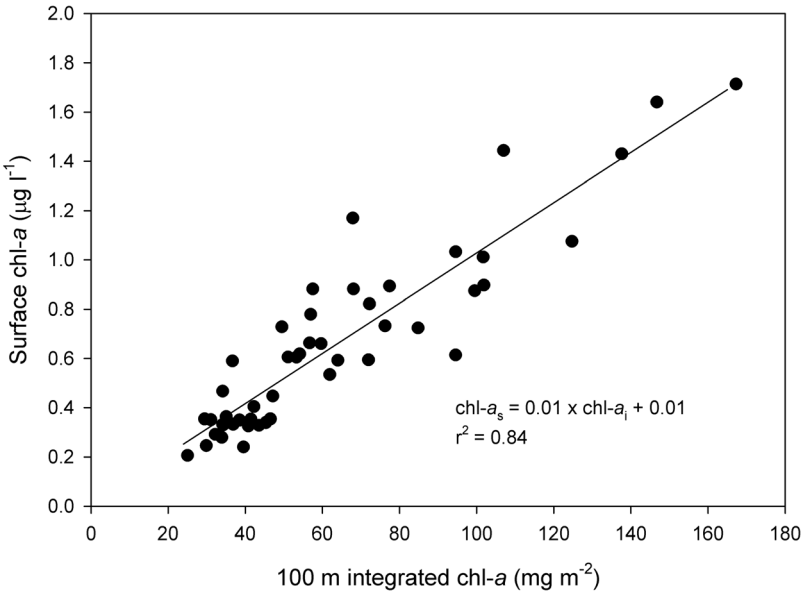

Figure 6. Relationship between surface (ca. 10 m) chl-*a* (chl-a_s) and 100 m integrated chl-*a* (chl-a_i).

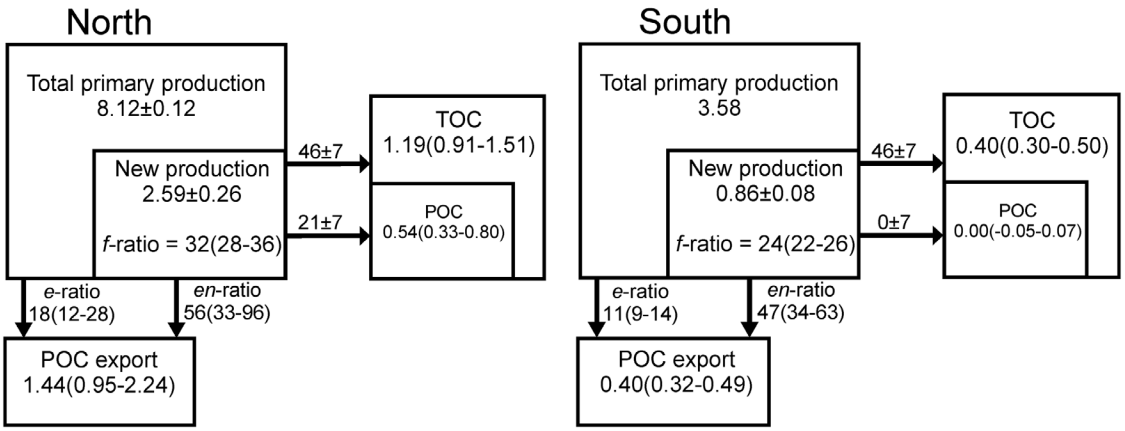

Figure 7. Schematic of the flow of organic carbon in the north and south regions. Values are in mol C m^{-2} measured up to the date of sampling. The ratios and fluxes between pools are percentages, with the fluxes into the TOC and POC pools taken from the regressions in Figure 5. Total primary production values are calculated regional averages, with a northern standard error from *Sanders et al.* [2007]; insufficient data are available to calculate a standard error in the south. NP values are the regional averages and standard errors calculated from the ΔNO_3^- data in Table S1 according to the method of *Sanders et al.* [2007]. Calculation of POC export and associated ranges is given in Table 2. All other ranges in parentheses are the maximum computational extremes.

[33] An interesting result from the carbon budget (Figure 7) are the traditional *f*-ratios, the ratio between new and total production [*Eppley and Peterson*, 1979], which are 32% and 24% in the northern and southern regions, respectively. Before the formation of the CROZEX carbon budget, *f*-ratios of >50% might typically be expected in high-latitude areas [*Lucas et al.*, 2007]. However, this expectation is built on instantaneous ^{15}N incubations, whereas these *f*-ratios are built on seasonal integrals. The low *f*-ratio of 24% in the south is typical of what is expected in low-latitude areas [*Yool et al.*, 2007], implying that a greater fraction of recycled nutrients are contributing to total primary production in the southern region.

[34] The *e*-ratio, defined as the fraction of total primary production that is exported as POC [*Murray et al.*, 1989], is 18% in the north compared to 11% in the south. Under these circumstances, and given that the *f*-ratios are greater than the *e*-ratios in, some proportion of NP must remain in the surface ocean and not be exported. This fraction, which is detectable in the TON and PON observations discussed in section 4 may be respired in situ after the bloom or exported later through other pathways such as lateral advection or winter mixing.

[35] The ratio between ΔNO_3^- NP and POC export can be summarized by a term known here as the *en*-ratio [*Morris*, 2008], which gives direct information on how much ΔNO_3^- NP is not being exported and thus how much organic material is accumulating as DOM and POM. The *en*-ratio in both regions is about 50% and highlights that approximately half of NP cannot be accounted for in particles exported over the time scale of the study. Instead a little over half of NP accumulates as DOM and POM in the mixed layer with the remainder then sinking as particles.

[36] The suggestion that NP and particulate export are not equivalent is somewhat controversial since a central tenet of biological oceanography is that the two terms are equivalent when analyzed over appropriate (i.e., large) time and space scales [*Dugdale and Goering*, 1967; *Eppley and Peterson*, 1979]. As far as possible, the CROZEX study and the analyses presented herein have tried to assess process occurring over the seasonal cycle, a point at which NP and particle export should approach balance.

[37] Therefore, arriving at a situation where only about 50% of NP can be accounted for in sinking particles in a high-latitude diatom dominated bloom is a surprising result. Given that a large fraction of the offset between new and export production is in the dissolved phase, which is unlikely to sink, and that sampling continued for a considerable period after the main bloom had occurred, it seems unlikely that all of this material will be exported via gravitational sinking. Possibly, it will be mixed down and recycled at depth in winter and therefore truly be exported, however the possibility exists that some of it may be recycled in the surface ocean and hence that NP, as traditionally estimated, does not equate to export production over large time and space scales.

[38] The major uncertainty in accepting this result revolves around whether the Si-scaling model is an appropriate way to integrate ^{234}Th-derived estimates of POC export. Here, the major concern is the possible impact of temporal variability in the Si:C ratios in exported particles, which may change over the course of the bloom as the effects of Fe limitation come into play [*Franck et al.*, 2000; *Hutchins and Bruland*, 1998; *Takeda*, 1998]. Fortunately, the alternative strategy adopted to determine the fate of NP in the surface ocean, namely the examination of the dissolved and particulate organic stocks, was successful in that it allowed an internally consistent carbon budget to be compiled (Figure 7).

5.2. Carbon to Iron Ratios

[39] This investigation of the CROZEX data set now provides strong evidence for greater seasonal export in the

northern Fe fertilized bloom region compared to the HNLC control site to the south. The quantitative ratio between Fe supply and POC export below the mixed layer is known as the sequestration efficiency (SE), calculated as the additional or excess POC exported, and Fe supplied, in the Fe enriched region when compared to the HNLC region. The SE is important because it is a fundamental parameter linking the supply of the biolimiting nutrient (Fe) to the key ecosystem function of POC export, and allows for cross comparison between different studies [*Buesseler and Boyd*, 2003].

[40] *Pollard et al.* [2009] estimated the SE by combining estimates of Fe supply from *Planquette et al.* [2007] and POC export estimates from an earlier iteration of the Si-scaling model. *Planquette et al.* [2007] calculated excess Fe using a steady state input of Fe from the surrounding plateau. Atmospheric and upwelling inputs are considered to be the same in both the bloom and nonbloom regions, which only leaves the horizontal export from the plateau as the term generating the excess Fe in the bloom region [*Charette et al.*, 2007; *Planquette*, 2008; *Planquette et al.*, 2007]. The horizontal flux of Fe from the plateau was estimated to be 390 nmol m^{-2} d^{-1}, which over 100 days of winter mixing and a mixed layer of 100 m, equates to 0.039 mmol m^{-2}. *Pollard et al.* [2009] estimated the excess POC export below 100 m to be 670 mmol C m^{-2} (Table S2 in the work of *Pollard et al.* [2009]) (960 − 289 = 670), and using a Martin curve [*Martin et al.*, 1987] with a *b* value of −0.99 extrapolated this to a POC excess of 337 mmol C m^{-2} at 200 m. The resultant SE is thus 17200 at 100 m or 8640 at 200 m.

[41] Following this, the SE calculated by *Pollard et al.* [2009] can now be updated in two ways. First, the refined Si-scaling model, which now includes a DSi upwelling component, now estimates the POC excess to be 1041 mmol C m^{-2} (Table 2, 1437 − 396 = 1041). Second, the *Pollard et al.* [2009] estimate did not consider the continuation of Fe input during the time of the bloom itself. If the input of Fe is considered to continue at the same prebloom rate from the start of the bloom (early September) until the peak of the bloom (late October), an additional 58 days (Figure 2), then an additional 0.023 mmol m^{-2} of Fe will be added to the Fe replete bloom area thus increasing the Fe excess to 0.062 mmol m^{-2}. This corresponds to a SE of about 16790 at 100 m, or 8450 at 200 m, similar to the *Pollard et al.* [2009] estimate. Thus the SE calculation remains little changed after the additional supplies of upwelled DSi and laterally advected Fe are updated. Although it should be pointed out that simultaneous alterations in both these terms do serve to cancel each other, giving rise to a little altered SE. One major uncertainty is the value of the *b* parameter used to extrapolate the estimate from 100 m to 200 m. It is simplistic to think that this is geographically invariant; indeed, *Lam and Bishop* [2007] have presented data suggesting that it may vary widely within a study area itself. Future research should focus on establishing the rate of recycling of sinking organic matter in this key depth range, a conclusion also reached by *Buesseler and Boyd* [2009].

[42] The SE of 8450 at 200 m is substantially lower than the seasonal SE estimated for KEOPS (668,000 [*Blain et al.*, 2007]). It is however similar to values of artificial Fe fertilization experiments in the Southern Ocean (average 4,300; range, 1,066–35,680 [*de Baar et al.*, 2005]). However, the SE for KEOPS has recently been reassessed after an updated Fe budget considered the lateral advection of Fe from the plateau of nearby Heard Island. When this additional source of Fe is factored into the KEOPS Fe budget the SE drops to 154,000; fourfold less than the original estimate by *Blain et al.* [2007], but is still 18-fold greater than the SE estimated for CROZEX [*Chever et al.*, 2010]. Consequently, major discrepancies in the SE still exist and will only be reconciled through further investigation.

6. Conclusions

[43] Presented here is a complete carbon budget study of the CROZEX bloom. The export estimates reported by *Pollard et al.* [2009], which are substantially lower than the NP estimates of *Sanders et al.* [2007] and *Lucas et al.* [2007] are validated by determining the magnitude of organic matter storage. The fraction of NP which is exported via gravitational sinking over the time scale of the study is approximately 50%. Finally, the CROZEX SE has been updated with a refined Si-scaling model and with a reconsideration of the Fe supply.

[44] **Acknowledgments.** CROZEX was a hugely multidisciplinary project and involved many different people, each of whom contributed to the large CROZEX data set. The authors wish to acknowledge the following people for their contributions: Ian Salter for analysis of SAPS BSi, Megan French for water column BSi, Mark Stinchcombe for nutrient analysis on D285, Sandy Thomalla for ^{234}Th analysis on D286, Mark Moore for chlorophyll analysis, Sophie Seeyave and Bob Head for POC analysis, and the filtering team Mike Lucas, Sophie Seeyave, and Robert Williamson for filtering POC/N, BSi, and chlorophyll. Mark Moore made helpful comments and suggestions that helped improve the manuscript, and discussions between Mark and R.S. helped develop the idea of the Si-scaling model. Two anonymous reviewers made extensive comments on the work that greatly improved the manuscript. Funding for CROZEX came from the NERC core strategic program BICEP. Many thanks to the crew of the RRS *Discovery* for D285 and D286.

References

Bakker, D. C. E. (1998) Process studies of the air-sea exchange of carbon dioxide in the Atlantic Ocean, Ph.D. thesis, Univ. of Groningen, Groningen, Netherlands.

Bakker, D. C. E., H. J. W. DeBaar, and U. V. Bathmann (1997), Changes of carbon dioxide in surface waters during spring in the Southern Ocean, *Deep Sea Res., Part II*, *44*(1–2), 91–127, doi:10.1016/S0967-0645(96)00075-6.

Bakker, D. C. E., et al. (2006), Matching carbon pools and fluxes for the Southern Ocean Iron Release Experiment (SOIREE), *Deep Sea Res., Part I*, *53*(12), 1941–1960, doi:10.1016/j.dsr.2006.08.014.

Bakker, D. C. E., M. C. Nielsdottir, P. J. Morris, J. Venables, and A. J. Watson (2007), The island mass effect and biological carbon uptake for the subantarctic Crozet Archipelago, *Deep Sea Res., Part II*, *54*(18–20), 2174–2190, doi:10.1016/j.dsr2.2007.06.009.

Blain, S., et al. (2007), Effect of natural iron fertilization on carbon sequestration in the Southern Ocean, *Nature*, *446*(7139), 1070–1074, doi:10.1038/nature05700.

Bode, A., M. Varela, M. Canle, and N. Gonzalez (2001), Dissolved and particulate organic nitrogen in shelf waters of northern Spain during spring, *Mar. Ecol. Prog. Ser.*, *214*, 43–54, doi:10.3354/meps214043.

Boyd, P. W. (2008), Implications of large-scale iron fertilization of the oceans: Introduction and synthesis, *Mar. Ecol. Prog. Ser.*, *364*, 213–218, doi:10.3354/meps07541.

Boyd, P. W., et al. (2000), A mesoscale phytoplankton bloom in the polar Southern Ocean stimulated by iron fertilization, *Nature*, *407*(6805), 695–702, doi:10.1038/35037500.

Boyd, P. W., et al. (2007), Mesoscale iron enrichment experiments 1993–2005: Synthesis and future directions, *Science*, *315*(5812), 612–617, doi:10.1126/science.1131669.

Broecker, W. S., and T.-H. Peng (1982), *Tracers in the Sea*, Eldigio, New York.

Brzezinski, M. A., and D. M. Nelson (1989), Seasonal changes in the silicon cycle within a Gulf Stream warm-core ring, *Deep Sea Res., Part A*, *36*(7), 1009–1030, doi:10.1016/0198-0149(89)90075-7.

Buesseler, K. O., and P. W. Boyd (2003), Will ocean fertilization work?, *Science*, *300*(5616), 67–68, doi:10.1126/science.1082959.

Buesseler, K. O., and P. W. Boyd (2009), Shedding light on processes that control particle export and flux attenuation in the twilight zone of the open ocean, *Limnol. Oceanogr.*, *54*(4), 1210–1232, doi:10.4319/lo.2009.54.4.1210.

Calvert, S. E. (1983), Sedimentary geochemistry of silicon, in *Silicon Geochemistry and Biogeochemistry*, edited by S. R. Aston, pp. 143–186, Academic, London.

Carlson, C. A., D. A. Hansell, E. T. Peltzer, and W. O. Smith (2000), Stocks and dynamics of dissolved and particulate organic matter in the southern Ross Sea, Antarctica, *Deep Sea Res., Part II*, *47*(15–16), 3201–3225, doi:10.1016/S0967-0645(00)00065-5.

Charette, M. A., M. E. Gonneea, P. J. Morris, P. Statham, G. Fones, H. Planquette, I. Salter, and A. N. Garabato (2007), Radium isotopes as tracers of iron sources fueling a Southern Ocean phytoplankton bloom, *Deep Sea Res., Part II*, *54*(18–20), 1989–1998, doi:10.1016/j.dsr2.2007.06.003.

Chever, F., G. Sarthou, E. Bucciarelli, B. Blain, and A. R. Bowie (2010), An iron budget during the natural iron fertilisation experiment KEOPS (Kerguelen Islands, Southern Ocean), *Biogeosciences*, *7*, 455–468, doi:10.5194/bg-7-455-2010.

Conan, P., et al. (2007), Partitioning of organic production in marine plankton communities: The effects of inorganic nutrient ratios and community composition on new dissolved organic matter, *Limnol. Oceanogr.*, *52*(2), 753–765, doi:10.4319/lo.2007.52.2.0753.

Dagg, M. J., J. Urban-Rich, and J. O. Peterson (2003), The potential contribution of fecal pellets from large copepods to the flux of biogenic silica and particulate organic carbon in the Antarctic Polar Front region near 170°W, *Deep Sea Res., Part II*, *50*(3–4), 675–691, doi:10.1016/S0967-0645(02)00590-8.

de Baar, H. J. W., et al. (2005), Synthesis of iron fertilization experiments: From the Iron Age in the Age of Enlightenment, *J. Geophys. Res.*, *110*, C09S16, doi:10.1029/2004JC002601.

DeMaster, D. J. (1981), The supply and accumulation of silica in the marine environment, *Geochim. Cosmochim. Acta*, *45*(10), 1715–1732, doi:10.1016/0016-7037(81)90006-5.

Discovery Reports (1929), *Discovery Investigations Station List 1925–1927*, *Discovery Rep.*, vol. 1, 140 pp., Cambridge Univ. Press, Cambridge, U. K.

Dugdale, R. C., and J. J. Goering (1967), Uptake of new and regenerated forms of nitrogen in primary productivity, *Limnol. Oceanogr.*, *12*(2), 196–206, doi:10.4319/lo.1967.12.2.0196.

Dugdale, R. C., F. P. Wilkerson, and H. J. Minas (1995), The role of a silicate pump in driving new production, *Deep Sea Res., Part I*, *42*(5), 697–719, doi:10.1016/0967-0637(95)00015-X.

Ehrhardt, M., and W. Koeve (1999), Determination of particulate organic carbon and nitrogen, in *Methods of Seawater Analysis*, 3rd ed., edited by K. Grasshoff, K. Kremling, and M. Ehrhardt, chap. 17, pp. 437–444, Wiley-VCH, Weinheim, Germany, doi:10.1002/9783527613984.ch17.

El-Sayed, S. Z., D. C. Biggs, and O. Holm-Hansen (1983), Phytoplankton standing crop, primary productivity, and near-surface nitrogenous nutrient fields in the Ross Sea, Antarctica, *Deep Sea Res., Part A*, *30*(8), 871–886, doi:10.1016/0198-0149(83)90005-5.

Eppley, R. W., and B. J. Peterson (1979), Particulate organic matter flux and planktonic new production in the deep ocean, *Nature*, *282*(5740), 677–680, doi:10.1038/282677a0.

Falkowski, P. G., R. T. Barber, and V. Smetacek (1998), Biogeochemical controls and feedbacks on ocean primary production, *Science*, *281*(5374), 200–206, doi:10.1126/science.281.5374.200.

Franck, V. M., M. A. Brzezinski, K. H. Coale, and D. M. Nelson (2000), Iron and silicic acid concentrations regulate Si uptake north and south of the Polar Frontal Zone in the Pacific Sector of the Southern Ocean, *Deep Sea Res., Part II*, *47*(15–16), 3315–3338, doi:10.1016/S0967-0645(00)00070-9.

Geider, R. J., and J. La Roche (1994), The role of iron in phytoplankton photosynthesis, and the potential for iron-limitation of primary productivity in the sea, *Photosynth. Res.*, *39*(3), 275–301, doi:10.1007/BF00014588.

Greene, R. M., R. J. Geider, and P. G. Falkowski (1991), Effect of iron limitation on photosynthesis in a marine diatom, *Limnol. Oceanogr.*, *36*(8), 1772–1782, doi:10.4319/lo.1991.36.8.1772.

Hilton, J., J. P. Lishman, S. Mackness, and S. I. Heaney (1986), An automated method for the analysis of 'particulate' carbon and nitrogen in natural waters, *Hydrobiologia*, *141*(3), 269–271, doi:10.1007/BF00014221.

Hoffmann, L. J., I. Peeken, K. Lochte, P. Assmy, and M. Veldhuis (2006), Different reactions of Southern Ocean phytoplankton size classes to iron fertilization, *Limnol. Oceanogr.*, *51*(3), 1217–1229, doi:10.4319/lo.2006.51.3.1217.

Holeton, C. L., F. Nedelec, R. Sanders, L. Brown, C. M. Moore, D. P. Stevens, K. J. Heywood, P. J. Statham, and C. H. Lucas (2005), Physiological state of phytoplankton communities in the southwest Atlantic sector of the Southern Ocean, as measured by fast repetition rate fluorometry, *Polar Biol.*, *29*(1), 44–52, doi:10.1007/s00300-005-0028-y.

Hu, S., and W. O. Smith (1998), The effects of irradiance on nitrate uptake and dissolved organic nitrogen release by phytoplankton in the Ross Sea, *Cont. Shelf Res.*, *18*(9), 971–990, doi:10.1016/S0278-4343(98)00021-1.

Hutchins, D. A., and K. W. Bruland (1998), Iron-limited diatom growth and Si: N uptake ratios in a coastal upwelling regime, *Nature*, *393*(6685), 561–564, doi:10.1038/31203.

Jacquet, S. H. M., F. Dehairs, N. Savoye, I. Obernosterer, U. Christaki, C. Monnin, and D. Cardinal (2008), Mesopelagic organic carbon remineralization in the Kerguelen Plateau region tracked by biogenic particulate Ba, *Deep Sea Res., Part II*, *55*(5–7), 868–879, doi:10.1016/j.dsr2.2007.12.038.

Kähler, P., P. K. Bjornsen, K. Lochte, and A. Antia (1997), Dissolved organic matter and its utilization by bacteria during spring in the Southern Ocean, *Deep Sea Res., Part II*, *44*(1–2), 341–353, doi:10.1016/S0967-0645(96)00071-9.

Kirkwood, D. (1996), Nutrients: Practical notes on their determination in sea water, *ICES Tech. Mar. Environ. Sci.*, *17*, 1–25.

Korb, R. E., M. J. Whitehouse, A. Atkinson, and S. E. Thorpe (2008), Magnitude and maintenance of the phytoplankton bloom at South Georgia: A naturally iron-replete environment, *Mar. Ecol. Prog. Ser.*, *368*, 75–91, doi:10.3354/meps07525.

Lam, P. J., and J. K. B. Bishop (2007), High biomass, low export regimes in the Southern Ocean, *Deep Sea Res., Part II*, *54*(5–7), 601–638, doi:10.1016/j.dsr2.2007.01.013.

Laws, E. A., P. G. Falkowski, W. O. Smith, H. Ducklow, and J. J. McCarthy (2000), Temperature effects on export production in the open ocean, *Global Biogeochem. Cycles*, *14*(4), 1231–1246, doi:10.1029/1999GB001229.

Ledford-Hoffman, P. A., D. J. DeMaster, and C. A. Nittrouer (1986), Biogenic silica accumulation in the Ross Sea and the importance of Antarctic continental shelf deposits in the marine silica budget, *Geochim. Cosmochim. Acta*, *50*(9), 2099–2110, doi:10.1016/0016-7037(86)90263-2.

Lucas, M., S. Seeyave, R. Sanders, C. M. Moore, R. Williamson, and M. Stinchcombe (2007), Nitrogen uptake responses to a naturally Fe-fertilised phytoplankton bloom during the 2004/2005 CROZEX study, *Deep Sea Res., Part II*, *54*(18–20), 2138–2173, doi:10.1016/j.dsr2.2007.06.017.

Martin, J. H., G. A. Knauer, D. M. Karl, and W. W. Broenkow (1987), VERTEX: Carbon cycling in the northeast Pacific, *Deep Sea Res., Part A*, *34*(2), 267–285, doi:10.1016/0198-0149(87)90086-0.

Moore, C. M., A. E. Hickman, A. J. Poulton, S. Seeyave, and M. I. Lucas (2007a), Iron-light interactions during the Crozet natural iron bloom and Export experiment (CROZEX): II. Taxonomic responses and elemental stoichiometry, *Deep Sea Res., Part II*, *54*(18–20), 2066–2084, doi:10.1016/j.dsr2.2007.06.015.

Moore, C. M., S. Seeyave, A. E. Hickman, J. T. Allen, M. I. Lucas, H. Planquette, R. T. Pollard, and A. J. Poulton (2007b), Iron-light interactions during the Crozet natural iron bloom and Export experiment (CROZEX): I. Phytoplankton growth and photophysiology, *Deep Sea Res., Part II*, *54*(18–20), 2045–2065, doi:10.1016/j.dsr2.2007.06.011.

Morris, P. J. (2008), Carbon export from natural iron fertilisation in the Southern Ocean, Ph.D. thesis, Univ. of Southampton, Southampton, U. K.

Morris, P. J., R. Sanders, R. Turnewitsch, and S. Thomalla (2007), ^{234}Th-derived particulate organic carbon export from an island-induced phytoplankton bloom in the Southern Ocean, *Deep Sea Res., Part II*, *54*(18–20), 2208–2232, doi:10.1016/j.dsr2.2007.06.002.

Mortlock, R. A., and P. N. Froelich (1989), A simple method for the rapid determination of biogenic opal in pelagic marine sediments, *Deep Sea Res., Part A*, *36*(9), 1415–1426, doi:10.1016/0198-0149(89)90092-7.

Murray, J. W., J. N. Downs, S. Strom, C. L. Wei, and H. W. Jannasch (1989), Nutrient assimilation, export production and ^{234}Th scavenging in the eastern equatorial Pacific, *Deep Sea Res., Part A*, *36*(10), 1471–1489, doi:10.1016/0198-0149(89)90052-6.

Nelson, D. M., and W. O. Smith (1986), Phytoplankton bloom dynamics of the western Ross Sea ice edge: II. Mesoscale cycling of nitrogen and silicon, *Deep Sea Res., Part A*, *33*(10), 1389–1412, doi:10.1016/0198-0149(86)90042-7.

Planquette, H. (2008) Iron biogeochemistry in the waters surrounding the Crozet Islands, Southern Ocean, Ph.D. thesis, Univ. of Southampton, Southampton, U. K.

Planquette, H., et al. (2007), Dissolved iron in the vicinity of the Crozet Islands, Southern Ocean, *Deep Sea Res., Part II*, *54*(18–20), 1999–2019, doi:10.1016/j.dsr2.2007.06.019.

Pollard, R. T., and R. Sanders (2006), RRS *Discovery* cruises 285/286, 3 Nov – 10 Dec 2004, 13 Dec 2004 – 21 Jan 2005: Crozet circulation, iron fertilization and Export production experiment (CROZEX), *Cruise Rep. 60*, Southampton Oceanogr. Cent., Southampton, U. K.

Pollard, R., R. Sanders, M. Lucas, and P. Statham (2007a), The Crozet natural iron bloom and EXport experiment (CROZEX), *Deep Sea Res., Part II*, *54*(18–20), 1905–1914, doi:10.1016/j.dsr2.2007.07.023.

Pollard, R. T., H. J. Venables, J. F. Read, and J. T. Allen (2007b), Large-scale circulation around the Crozet Plateau controls an annual phytoplankton bloom in the Crozet Basin, *Deep Sea Res., Part II*, *54*(18–20), 1915–1929, doi:10.1016/j.dsr2.2007.06.012.

Pollard, R. T., et al. (2009), Southern Ocean deep-water carbon export enhanced by natural iron fertilization, *Nature*, *457*(7229), 577–580, doi:10.1038/nature07716.

Prentice, I. C., G. D. Farquhar, M. J. R. Fasham, M. L. Goulden, M. Heimann, V. J. Jaramillo, H. S. Kheshgi, C. Le Quéré, R. J. Scholes, and D. W. R. Wallace (2001), The carbon cycle and atmospheric carbon dioxide, in *Climate Change 2001: The Scientific Basis. Contributions of Working Group I to the Third Assessment Report of the International Panel on Climate Change*, edited by J. T. Houghton et al., chap. 3, pp. 183–237, Cambridge Univ. Press, Cambridge, U. K.

Rutgers van der Loeff, M. M., and W. S. Moore (1999), Determination of natural radioactive tracers, in *Methods of Seawater Analysis*, edited by K. Grasshoff, K. Kremling, and M. Ehrhardt, chap. 13, pp. 365–398, Wiley-VCH, Weinheim, Germany.

Salter, I. (2007), Particle fluxes in the north-east Atlantic and the Southern Ocean, Ph.D. thesis, Univ. of Southampton, Southampton, U. K.

Salter, I., R. S. Lampitt, R. Sanders, A. Poulton, A. E. S. Kemp, B. Boorman, K. Saw, and R. Pearce (2007), Estimating carbon, silica and diatom export from a naturally fertilised phytoplankton bloom in the Southern Ocean using PELAGRA: A novel drifting sediment trap, Deep Sea Res., Part II, 54(18–20), 2233–2259, doi:10.1016/j.dsr2.2007.06.008.

Sanders, R., and T. Jickells (2000), Total organic nutrients in Drake Passage, *Deep Sea Res., Part I*, *47*(6), 997–1014, doi:10.1016/S0967-0637(99)00079-5.

Sanders, R., L. Brown, S. Henson, and M. Lucas (2005), New production in the Irminger Basin during 2002, *J. Mar. Syst.*, *55*(3–4), 291–310, doi:10.1016/j.jmarsys.2004.09.002.

Sanders, R., P. J. Morris, M. Stinchcombe, S. Seeyave, H. Venables, and M. Lucas (2007), New production and the *f* ratio around the Crozet Plateau in austral summer 2004–2005 diagnosed from seasonal changes in inorganic nutrient levels, *Deep Sea Res., Part II*, *54*(18–20), 2191–2207, doi:10.1016/j.dsr2.2007.06.007.

Savoye, N., T. W. Trull, S. H. M. Jacquet, J. Navez, and F. Dehairs (2008), ^{234}Th-based export fluxes during a natural iron fertilization experiment in the Southern Ocean (KEOPS), *Deep Sea Res., Part II*, *55*(5–7), 841–855, doi:10.1016/j.dsr2.2007.12.036.

Seeyave, S., M. I. Lucas, C. M. Moore, and A. J. Poulton (2007), Phytoplankton productivity and community structure in the vicinity of the Crozet Plateau during austral summer 2004/2005, *Deep Sea Res., Part II*, *54*(18–20), 2020–2044, doi:10.1016/j.dsr2.2007.06.010.

Small, L. F., S. W. Fowler, and M. Y. Unlu (1979), Sinking rates of natural copepod fecal pellets, *Mar. Biol. Berlin*, *51*(3), 233–241, doi:10.1007/BF00386803.

Smith, W. O., and L. I. Gordon (1997), Hyperproductivity of the Ross Sea (Antarctica) polynya during austral spring, *Geophys. Res. Lett.*, *24*(3), 233–236, doi:10.1029/96GL03926.

Smith, W. O., D. M. Nelson, G. R. DiTullio, and A. R. Leventer (1996), Temporal and spatial patterns in the Ross Sea: Phytoplankton biomass, elemental composition, productivity and growth rates, *J. Geophys. Res.*, *101*(C8), 18,455–18,465, doi:10.1029/96JC01304.

Sweeney, C., et al. (2000), Nutrient and carbon removal ratios and fluxes in the Ross Sea, Antarctica, *Deep Sea Res., Part II*, *47*(15–16), 3395–3421, doi:10.1016/S0967-0645(00)00073-4.

Takeda, S. (1998), Influence of iron availability on nutrient consumption ratio of diatoms in oceanic waters, *Nature*, *393*(6687), 774–777, doi:10.1038/31674.

Tande, K. S. (1985), Assimilation efficiency in herbivorous aquatic organisms: The potential of the ratio method using ^{14}C and biogenic silica as markers, *Limnol. Oceanogr.*, *30*(5), 1093–1099, doi:10.4319/lo.1985.30.5.1093.

Tréguer, P., and G. Jacques (1986), The Antarctic Ocean, *Recherche*, *17*(178), 746–755.

Tréguer, P., D. M. Nelson, A. J. Vanbennekom, D. J. DeMaster, A. Leynaert, and B. Quéguiner (1995), The silica balance in the world ocean: A reestimate, *Science*, *268*(5209), 375–379, doi:10.1126/science.268.5209.375.

Venables, H. J., R. T. Pollard, and E. E. Popova (2007), Physical conditions controlling the development of a regular phytoplankton bloom north of the Crozet Plateau, Southern Ocean, *Deep Sea Res., Part II*, *54*(18–20), 1949–1965, doi:10.1016/j.dsr2.2007.06.014.

Verardo, D. J., P. N. Froelich, and A. McIntyre (1990), Determination of organic carbon and nitrogen in marine sediments using the Carlo Erba NA-1500 Analyzer, *Deep Sea Res., Part A*, *37*(1), 157–165, doi:10.1016/0198-0149(90)90034-S.

Welschmeyer, N. A. (1994), Fluorometric analysis of chlorophyll *a* in the presence of chlorophyll *b* and pheopigments, *Limnol. Oceanogr.*, *39*(8), 1985–1992, doi:10.4319/lo.1994.39.8.1985.

Wilson, D. L., W. O. Smith, and D. M. Nelson (1986), Phytoplankton bloom dynamics of the western Ross Sea ice edge: I. Primary productivity and species specific production, *Deep Sea Res., Part A*, *33*(10), 1375–1387, doi:10.1016/0198-0149(86)90041-5.

Yool, A., A. P. Martin, C. Fernandez, and D. R. Clark (2007), The significance of nitrification for oceanic new production, *Nature*, *447*(7147), 999–1002, doi:10.1038/nature05885.

Zubkov, M. V., R. J. Holland, P. H. Burkill, I. W. Croudace, and P. E. Warwick (2007), Microbial abundance, activity and iron uptake in vicinity of the Crozet Isles in November 2004–January 2005, *Deep Sea Res., Part II*, *54*(18–20), 2126–2137, doi:10.1016/j.dsr2.2007.06.020.

P. J. Morris, Department of Marine Chemistry and Geochemistry, Woods Hole Oceanographic Institution, 266 Woods Hole Road, Woods Hole, MA 02543, USA. (pmorris@whoi.edu)

R. Sanders, National Oceanography Centre, Southampton, University of Southampton, European Way, Southampton, SO14 3ZH, UK.